Effect of GBCD on IGC susceptibility of solution treated 2024 Al alloy

G P Li, C L He[1], R Li, J M Shi, G F Ma, X Y Fu, H Z Chen and J M Wang

Liaoning Provincial Key Laboratory of Advanced Materials, Shenyang University, Shenyang 110044, China

[1] E-mail: ccllhhe@126.com

Abstract. Grain boundary character distribution (GBCD) of solution heat treated 2024 Al alloy was analyzed by electron backscattered diffraction, and intergranular corrosion (IGC) susceptibility and corrosion weight loss of the 2024 Al were investigated according to ASTM G110-92. The grain boundaries are composed of 12.17% low angle (∑1) boundaries, 10.87% low coincidence site lattice (∑3-∑29) boundaries and 76.96% random (R) boundaries. After corrosion for 6 h, the corroded boundary proportions of ∑1, ∑3, ∑5-∑29 and R boundaries were 10.71%, 11.11%, 21.95% and 25.14%, respectively. This shows that the GBCD has a great effect on IGC susceptibility of the solution treated 2024 Al, and both ∑1 and ∑3 boundaries exhibit much higher IGC resistance than ∑5-∑29 and R boundaries. Among all the boundaries, the R boundaries have the highest IGC susceptibility.

1. Introduction

In 1984, Watanabe [1] proposed the concept of grain boundary character distribution (GBCD) which is a parameter used to quantitatively describe the type and frequency of grain boundaries present in a microstructure. On the basis of coincidence site lattice (CSL) model, the grain boundaries are divided into low angle (∑1) boundaries, low ∑CSL grain boundaries (Σ≤29) and random grain boundaries (R). The R type boundaries refer to the general high-angle boundaries and the CSL grain boundaries of Σ > 29. Kim et al [2] found that IGC susceptibility of pure aluminum in HCl solution was strongly dependent on its GBCD. In 8%, 16% and 38% HCl, the IGC resistance of the ∑1 boundary was the best. In 8% and 16% HCl, the ∑3 grain boundary exhibited higher IGC resistance compared with the R boundaries. In NiAl intermetallic compound [3], the ∑1, ∑3 and ∑5 boundaries could obviously prevent the continuation of cracks, while ∑7, ∑11, ∑13, ∑21 and ∑23 grain boundaries had a relatively poor ability to prevent crack continuity. Meng et al [4] found that the selective features of IGC in Al alloy and Al matrix composites were mainly related to GBCD. High-angle boundaries were easy to be attacked while special grain boundary and low angle boundary had high IGC resistance [5].

In this paper, solution heat treated 2024 Al alloy was chosen as the research material and the relationship between GBCD and IGC susceptibility was studied in detail.

2. Materials and methods

The material used in this study was as rolled plates of 2024 Al alloy, its chemical composition was listed in table 1. Samples were solution heat treated in an air circulation furnace at 495 ±3 ℃ for 40 min and then cooled in air immediately. The sample dimensions were about 10 mm × 5 mm × 1 mm. The test samples were successively ground on emery papers from 400# to 2000#, and then polished by

1.0 μm diamond paste. After that, the samples were electropolished in an electrolyte containing 10 vol % $HClO_4$ + 90 vol % ethanol for 7 s under a DC voltage of 29 V, the electrolyte temperature was less than 10 ºC. Stainless steel plate was selected as the cathode.

Table 1. The chemical composition of 2024 Al alloy (mass fraction, %).

Element	Cu	Mg	Mn	Fe	Si	Zn	Ti	Ni	Al
Content	3.8~4.9	1.2~1.8	0.3~0.9	0.5	0.5	0.3	0.1	0.1	Bal.

The GBCD data of the solution treated 2024 Al sample were obtained by using Hitachi S-4800 field emission scanning electron microscope equipped with EBSD detector and Oxford's CHANEL5 HKL. The tested area was automatically scanned with a step size of 2.5 μm. The distribution of grain size was obtained by the supporting software. The IGC experiments were carried out according to ASTM G 110-92, which involved degreasing in acetone and ethanol, immersion etching (1 min in 945 mL H_2O+50 mL HNO_3+5 mL HF at 93℃), rinsing in reagent water, immersion in concentrated nitric acid (70 %) for 1 min, and rinsing in reagent water and air dry, followed by 6 h immersion in solution (57 g NaCl and 10 mL H_2O_2 per litre) 30 ℃. The corrosion morphology was observed by a metallographic microscope, and corrosion weight loss was measured by an electron balance with a precision of 0.1 mg.

3. Results and discussion

Figure 1a presents the grain size distribution of the solution heat treated 2024 Al (296 grains characterized), which shows that the distribution of grain sizes is non-uniform in the microstructure. The average grain size is 12.1 μm. The smallest grain size is 2.8 μm, and the largest is 81.1 μm. Thereinto, the fraction of grains with size between 2-4 μm is about 40% while grains greater than 40 μm is only about 7.1%. Figure 1b presents the misorientation angle distribution of the grain boundaries in the solution heat treated 2024 Al. In 460 grain boundaries characterized, the fractions of low angle (∑1) boundaries with misorientation angles less than 15 º and R (∑>29) boundaries are 12.17% and 76.96%, respectively, whereas the total fraction of low ∑ CSL (∑3-∑29) boundaries is 10.87%. Except 1.96% ∑3, the fraction of the other type CSL boundaries (∑5-∑29) is less than 8.91%.

Figure 2a shows the EBSD map of the 2024 Al alloy before corrosion test, and figure 2b presents the corrosion morphology in the same area after 6 h corrosion. This figure clearly demonstrates that many random boundaries have been seriously attacked while ∑5-∑29 boundaries are only a small amount of corrosion. The ∑1 and ∑3 boundaries are resistant to corrosion. Among them, the two ∑1 boundaries are not corroded. Because the connectivity of random grain boundaries is interrupted by the low ∑CSL grain boundaries and low angle boundaries, the IGC is non-uniform. Additionally, figure 1b also clearly shows that serious pitting corrosion took place in the sample. The corrosion mechanism of IGC results from galvanic corrosion between grain boundary precipitates (e.g. Al_2Cu) and Cu-depleted zone, while pitting can be contributed to galvanic corrosion between secondary phase particles (AlCuFeMnSi phase [6]) and matrix Al.

Figure 3 shows the fractions of each type grain boundaries and corroded grain boundaries in the sample. After corrosion 6 h, the corroded proportions of ∑1, ∑3, ∑5-∑29 and R boundaries are 10.71%, 11.11%, 21.95% and 25.14%, respectively. Obviously, both the ∑1 and ∑3 grain boundaries reveal much lower IGC susceptibility, which is associated with their lower energies of grain boundaries, and less impurity segregation in the boundaries. Compared with the ∑1 and ∑3 grain boundaries, much more ∑5-∑29 grain boundaries are attacked. In all the boundaries, the number of R boundaries attacked is the most. This shows that the GBCD has a great effect on IGC susceptibility of the solution treated 2024 Al. In general, ∑1 and ∑3 (twin) boundaries possesses the lowest energy in all the grain boundaries, therefore, they should exhibit the best IGC resistance. Low ∑CSL grain boundaries have higher structural order, relative low grain boundary energy and less boundary precipitation [7]; therefore, their IGC resistance is relative good although it is much lower than ∑1 and ∑3 boundaries. Because R grain boundaries have the highest boundary energies, they present the

lowest IGC resistance. The sequence of IGC susceptibility from low to high is: $\sum 1 \leq \sum 3 < \sum 5-\sum 29 <$ R. The proportion of corrosion boundaries in 460 grain boundaries characterized is 22.83%.

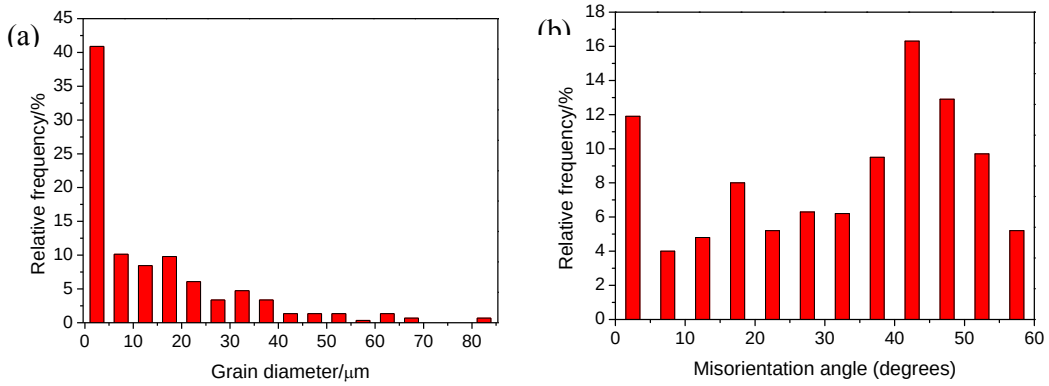

Figure 1. (a) Grain size distribution and (b) misorientation angle distribution for the 2024 Al alloy.

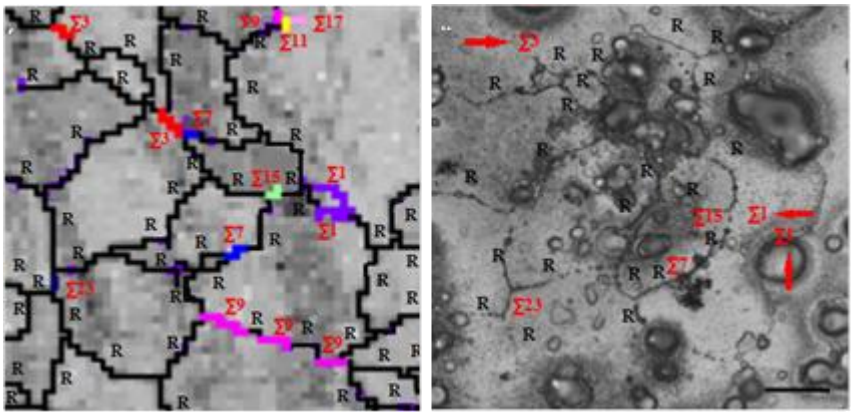

Figure 2. (a) EBSD map and (b) corrosion morphology of the sample before (a) and (b) after corrosion.

Figure 4 presents the change of weight loss with corrosion time. It is clearly shown that the weight loss is increased with corrosion time. However the corrosion rate is decreased with increasing time because the corrosion products covered on the sample surface, hindering the corrosion progress. When corrosion time increases from 1 h to 6 h, the corrosion rate of the 2024 Al alloy decreases from 18.91 mm/a to 17.86 mm/a.

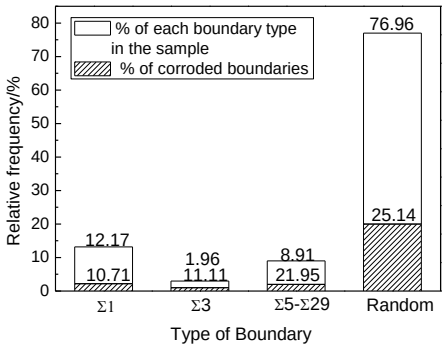

Figure 3. The relationship between GBCD and IGC susceptibility.

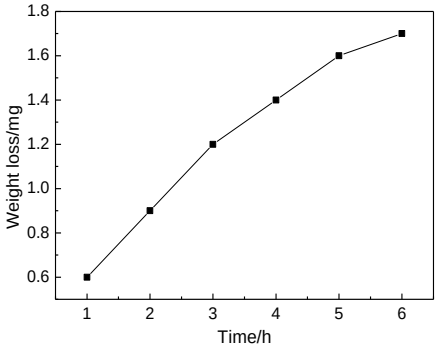

Figure 4. Weight loss vs corrosion time.

4. Conclusion

The GBCD of solution heat treated 2024 Al alloy was examined by EBSD, and IGC susceptibility and corrosion weight loss of the 2024 Al alloy were investigated according to ASTM G110-92. The average grain size of the 2024 Al alloy was 12.1 μm. The fractions of ∑1, ∑3, ∑5-∑29 and R grain boundaries in the sample were 12.17%, 1.96%, 8.91% and 76.96%, respectively. After corrosion for 6 h, the corroded boundary proportions of ∑1, ∑3, ∑5-∑29 and R boundaries were 10.71%, 11.11%, 21.95% and 25.14%, respectively. This showed that the GBCD had a great effect on IGC susceptibility of the solution treated 2024 Al alloy, and both ∑1 and ∑3 boundaries exhibited much better IGC resistance than ∑5-∑29 and R boundaries. Among all the boundaries, the R boundaries had the highest IGC susceptibility.

Acknowledgments

This work was financially supported by the Project-sponsored by SRF for ROCS, SEM and the National Natural Science Foundation (No. 51171118) of China.

References

[1] Watanabe T 1984 An approach to grain boundary design of strong and ductile polycrystals *Res Mechanica* **11** 47-84
[2] Kim S H, Erb U, Aust K T and Palumbo G 2001 Grain boundary character distribution and intergranular corrosion behavior in high purity aluminum *Scripta Materialia* **44** 835-839
[3] Kim T, Hong K T and Lee K S 2003 The relationship between the fracture toughness and grain boundary character distribution in polycrystalline *NiAl Intermetallics* **11** 33-39
[4] Meng C, Zhang D, Zhuang L and Zhang J 2016 Correlations between stress corrosion cracking grain boundary precipitates and Zn content of Al–Mg–Zn alloys *Journal of Alloys & Compounds* **655** 178-187
[5] Guérin M, Alexis J, Andrieu E, Laffont L, Lefebvre W and Odemer G 2016 Identification of the metallurgical parameters explaining the corrosion susceptibility in a 2050 aluminium alloy *Corrosion Science* **102** 291-300
[6] He C L, Lv S, Bai Y Y, Li R, Xie L P, Ma G F and Wang J M 2016 Effect of quenching methods on corrosion behavior of 2024 Al alloy *Journal of Shenyang University (Natural Science)* **28** 87-91
[7] Yuan X Y and Chen L Q 2016 Effect of grain and grain boundary features on anti-corrosion ability of a high manganese austenitic TWIP steel *Acta Metallurgica Sinica* **52** 1345-1352